Proceedings of the Institute of Acoustics

A SIMPLE MODEL OF HORN COVERAGE ANGLE

KR Holland ISVR, University of Southampton, UK
PR Newell Acoustics Consultant, Moaña, Spain

1 INTRODUCTION

Tools for predicting the performance or behaviour of loudspeaker horns can save a lot of time and other resources which would otherwise be spent on building and testing prototypes. In 1989 and 1991, the authors published the results of research carried out on the prediction and measurement of the one-parameter behaviour of horns [1, 2]. The one-parameter term, here, refers to a model of the sound field within a horn which consists (only) of pseudo-plane-waves, such that the spatial distribution of sound within the horn is a function only of the position along the horn axis (the one parameter). The work resulted in an efficient and compact method for predicting the acoustic impedance at the throat of a horn which was verified against measurements taken of the throat impedance of a wide variety of horns. Knowledge of the throat impedance allows further predictions of sound power output when a known source is attached to the throat (usually a compression driver) using a form of two-port network model [3]. However, the one-parameter description cannot be used to determine the directivity of the horn, and without this the sound power output cannot be converted into an on-axis sound pressure level or frequency response. Predictions of directivity would require 2- or 3-dimensional numerical models [4], such as finite element or boundary element models, which are computationally expensive. This paper describes an efficient and compact method for estimating the coverage angle of the sound emitted from a horn of arbitrary shape.

2 POWER OUTPUT, COVERAGE ANGLE AND ON-AXIS RESPONSE

The product of the mean-square volume velocity (q) of a source and the real part of the acoustic impedance at the throat of a horn (Z_T) yields the total sound power injected into the horn by the source,

$$W_S = \frac{|q|^2}{2} \Re\{Z_T\} \quad . \tag{1}$$

Assuming that the horn walls are perfectly rigid, and that sound absorption by the air in the horn is negligible, the sound power radiated from the mouth of the horn will be equal to that injected by the source.

The coverage angle (θ_C) of a horn is defined as twice the angle away from the axis at which the sound pressure is half of the sound pressure on the axis (the 6dB-down angle). If there is only one major lobe in the directivity pattern of the horn (valid for most 'good' loudspeaker horns), the on-axis pressure and the sound power can be approximately related by assuming that all of the radiated sound power is contained within the coverage angle. In addition, when horns are arrayed, the -6dB angle defines the overlap angle necessary to maintain continuous coverage. For example, if the horn is axi-symmetric with a circular cross-section, the on-axis mean-squared pressure is found by considering the sound intensity passing through a spherical cap with a polar angle equal to half the horn coverage angle

$$\frac{|p_0|^2}{2} \approx \frac{\rho c W_S}{2\pi r^2\left(1-\cos\left({}^{\theta_C}/_{2}\right)\right)}, \tag{2}$$

where r is the distance from the horn to the point at which the pressure is required. For a rectangular cross-section horn, the coverage angle is different in the two axes in general, and the on-axis pressure can be approximated by

$$\frac{|p_0|^2}{2} \approx \frac{\rho c W_S}{r^2 \theta_H \theta_V}, \tag{3}$$

where θ_H and θ_V are the horizontal and vertical coverage angles respectively.

3 A SIMPLE MODEL OF HORN COVERAGE ANGLE

3.1 The Piston Directivity Function

The key ingredient in the horn coverage angle model presented here is the 'piston directivity function'. This function describes the far-field directivity of a piston mounted in an otherwise continuous rigid baffle [5]. For a circular piston of radius a, this takes the form

$$D(\theta) = \frac{2J_1[ka\,sin(\theta)]}{ka\,sin(\theta)}, \tag{4}$$

where J_1 is the Bessel function of the 1st kind of order 1, θ is the angle away from the axis, and k is the wavenumber ($2\pi f/c$). Examples of this function for different values of ka are shown in Figure 1.

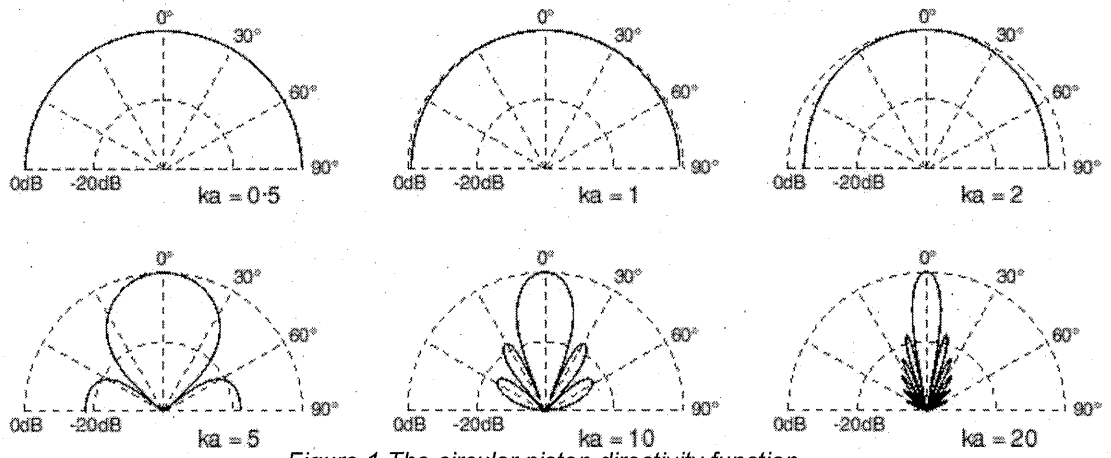

Figure 1 The circular piston directivity function.

By definition, the coverage angle of the piston is then evaluated as the angle and frequency at which the piston directivity function is equal to 0.5.

Rectangular pistons generally have different directivities along the two axes and the far-field directivity function is given by [5],

$$D(\theta_H\theta_V) = \frac{sin(kH\,sin(\theta_H))}{kHsin(\theta_H)} \frac{sin(kVsin(\theta_V))}{kVsin(\theta_V)}, \tag{5}$$

where H and V are half of the horizontal and vertical dimensions of the piston. The coverage angle is generally different in the two planes and these have similar shapes to those for the circular piston shown in Figure 1.

The directivity of pistons with elliptical or oval cross-section can be approximated by using the circular piston directivity function, with different values of a in the two planes,

$$D(\theta_H, \theta_V) = \frac{2J_1[ka_H sin(\theta_H)]}{ka_H sin(\theta_H)} \frac{2J_1[ka_V sin(\theta_V)]}{ka_V sin(\theta_V)} \quad , \tag{6}$$

3.2 Idealised Directivity of a Horn

The idealised directivity of horn loudspeakers has been covered in the literature [6, 7] and is the basis for the model described here.

Figure 2 shows the idealised coverage angle of a conical horn as a function of frequency. Three distinct frequency ranges are evident: a low-frequency range, determined by the size of the horn mouth; a mid-frequency range, determined by the horn walls; and a high-frequency range determined by the size of the throat [4, 6, 7, 8]. A reasonable explanation for these different frequency ranges can be found by considering the relationships between the wavelength of sound and the dimensions of the horn as the frequency is lowered from a very high frequency.

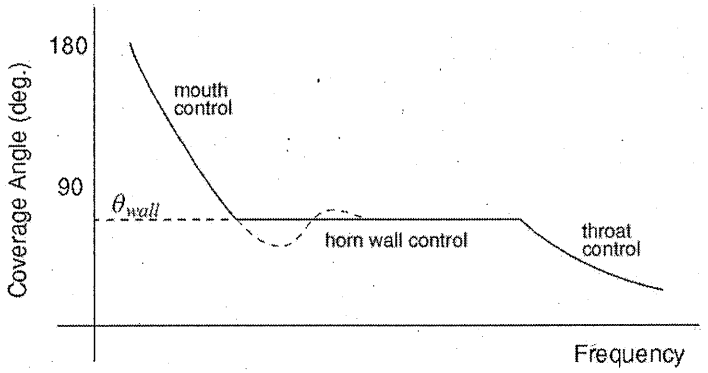

Figure 2 Idealised coverage angle of a straight-walled (or conical) horn showing three distinct frequency ranges

3.2.1 High-frequency range

At very high frequencies, where wavelengths are small compared to the throat of the horn (high 'ka' values in Figure 1), the throat of the horn beams the sound over an angle which is narrower than the horn walls, so that the walls have little effect, and the sound radiated can be approximated by that of a piston having the same dimensions as the throat (the 'throat piston'). In this frequency range, the coverage angle steadily widens as frequency is lowered, according to the piston directivity function (Eqs 4, 5, 6).

3.2.2 Mid-frequency range

When the frequency is lowered to a value for which the coverage angle for the throat piston is greater than the angle of the horn walls at the throat, the sound cannot propagate through the walls, so the radiation is constrained within the angle of the walls. As the wave propagates along the horn, it reaches a point in the horn where a virtual piston having the same dimensions as the horn at that axial position has the same coverage angle as the angle of the walls at that position; radiation from that point onwards is unconstrained by the horn walls and the coverage angle of the horn is fixed to be the angle of the horn walls at that position. As frequency is lowered further, the position within the horn where the coverage angle is set moves further down the horn until it reaches the mouth.

3.2.3 Low-frequency range

As frequency is lowered further, the wavelength becomes large compared to the mouth of the horn, and the sound radiated by the horn can be approximated by that of a piston having the same dimensions as the mouth. In this frequency range, the interior shape of the walls of the horn have little effect on the coverage angle, which steadily broadens as frequency is lowered, until it reaches 180 degrees.

3.2.4 Mouth narrowing effect

At frequencies around where the transition from mouth control to wall control occurs, the mouth does not behave very much like a piston, and diffraction effects, which are particular to the detailed geometry of the horn mouth, give rise to side-lobes in the directivity which serve to narrow the width of the main lobe and hence the coverage angle [6, 7]. The dotted line in Figure 2 serves to illustrate the typical effect of this coverage angle. Horns with wide flares at the mouth tend to be less prone to this narrowing than those having sharper transitions.

3.3 The Model

For a horn with straight or conical sides, the description of horn coverage angle in Section 3.2 is simple to implement as all of the angles within the mid-frequency range (Section 3.2.2) are the same. We thus have a frequency range of 'constant directivity'; so we need only the throat and mouth dimensions and the angle of the horn walls to build a full model. However, when a horn has multiple wall angles, or a curved, flaring profile, the model must be extended to include the detailed shape of the horn wall profile. The argument presented in Section 3.2.2 suggests that at any given frequency within the mid-frequency range, there is a unique position within the horn where the angle of the horn walls is equal to the coverage angle of a virtual piston having the same size as the horn flare at that position. That angle is then an approximation to the coverage angle of the horn at that frequency. Figure 3 illustrates this.

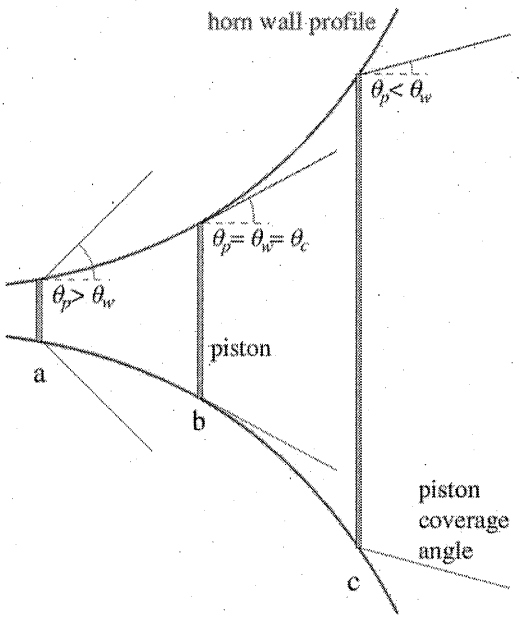

Figure 3 graphical illustration of relationship between the horn wall angle and the coverage angle of virtual pistons at three positions within the horn. The virtual piston at position b sets the horn coverage angle at that frequency.

This method can be implemented by dividing the horn wall into finite-length sections, or elements, similar to the method described in references [1 and 2]. The piston coverage angle in the centre of each element at the frequency of interest is compared to the corresponding horn wall angle until a close match is found; the horn coverage angle at that frequency is then that same angle.

4 COMPARISON WITH MEASURED DATA

At the same time as the one-parameter horn measurements [1, 2], other acoustic properties of a variety of horns were measured, including off-axis frequency responses [9]. These data are used here to validate the coverage angle model described in Section 3.3. Data for one axisymmetric horn and two horns with rectangular cross-sections are studied and compared with the model predictions based on the flare geometry.

Figures 3a and 3b show contour plots of the horizontal and vertical off-axis frequency responses of the rectangular exponential horn pictured in Figure A1 in the appendix. In these plots, the responses are normalised to the on-axis response, and the relative levels are plotted as a colour scale which is a function of frequency and angle. The levels corresponding to the colours are shown on the right of the plot, and the outputs of the horn coverage-angle model are shown on the same plots as solid black lines.

The agreement between the measurements and the model predictions is seen to be reasonably good, with the prediction lining up with the -6dB contour for much of the frequency range. An exception to this is the narrowing of the measured coverage angle at frequencies just above the mouth-control frequency range, as described in Section 3.2.4 and shown in Figure 2. Clearly, the model would need to include this effect if accuracy in this frequency range is required, but it should be noted here that the measurements were taken with the horns mounted on a finite-sized baffle, whereas the model assumes an infinite baffle.

Figures 4a and b are as Figures 3a and b, but for the rectangular sectoral horn pictured in Figure A2 in the appendix. This horn is characterised by several discontinuities within the flare, such as sharp edges and thick strengthening pillars. These features give rise to the uneven frequency responses and directivity, particularly in the horizontal plane, shown in Figure 4. These features are not modelled so do not affect the predictions. Apart from these features, the model predictions are reasonably accurate over much of the frequency range.

Comparing Figures 3a and 4a, the straight sides of the sectoral horn do give a wide frequency-range of constant, wide, directivity; in contrast to the narrowing coverage-angle with rising frequency of the exponential horn due to the flaring walls.

Figure 5 shows the directivity of the axisymmetric horn pictured in Figure A3, in the appendix. Agreement between the coverage-angle predictions and the -6dB contour are again reasonable.

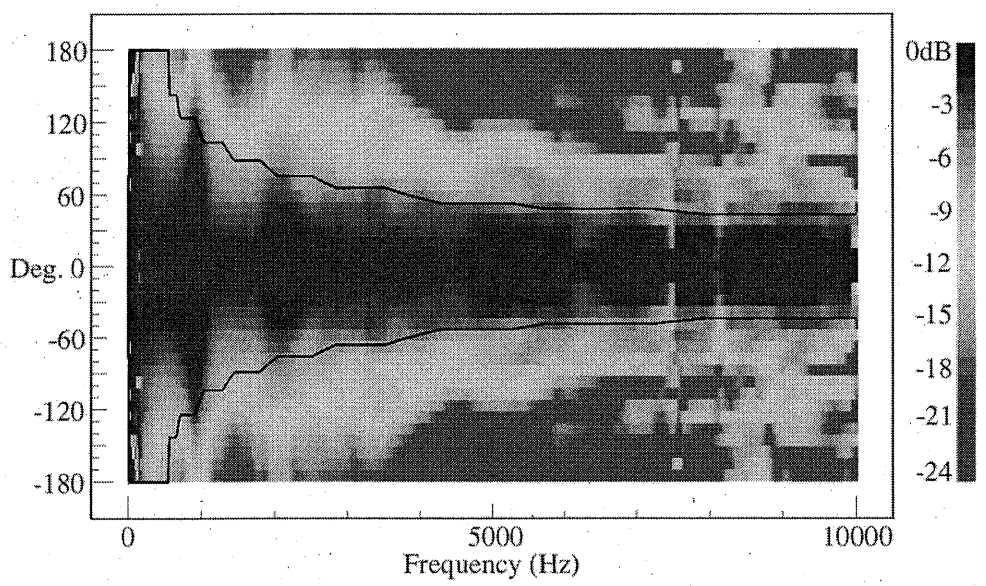

Figure 3a Measured horizontal off-axis frequency responses (colour contours) compared to model coverage-angle predictions (solid black lines): rectangular exponential horn

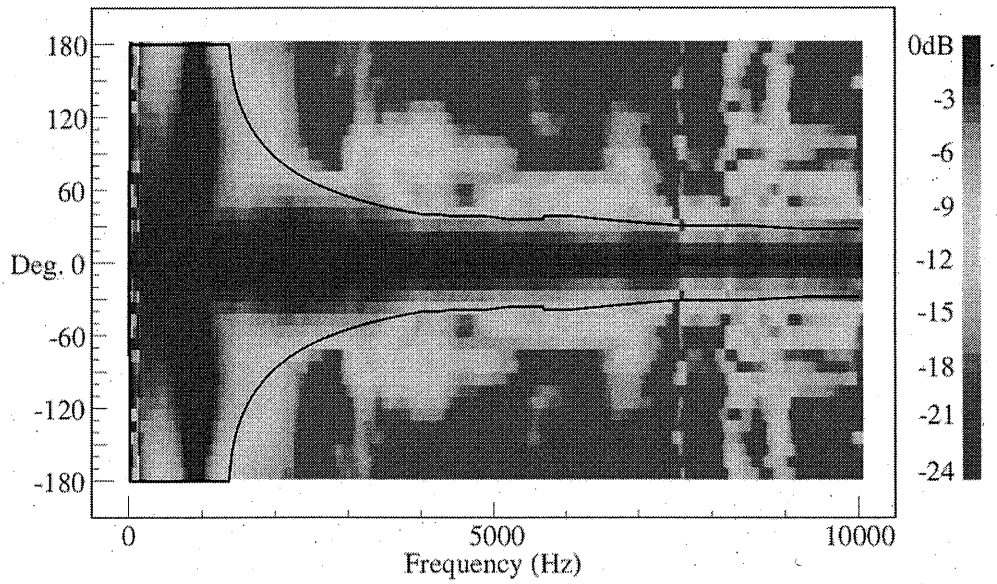

Figure 3b Measured vertical off-axis frequency responses (colour contours) compared to model coverage-angle predictions (solid black lines): rectangular exponential horn

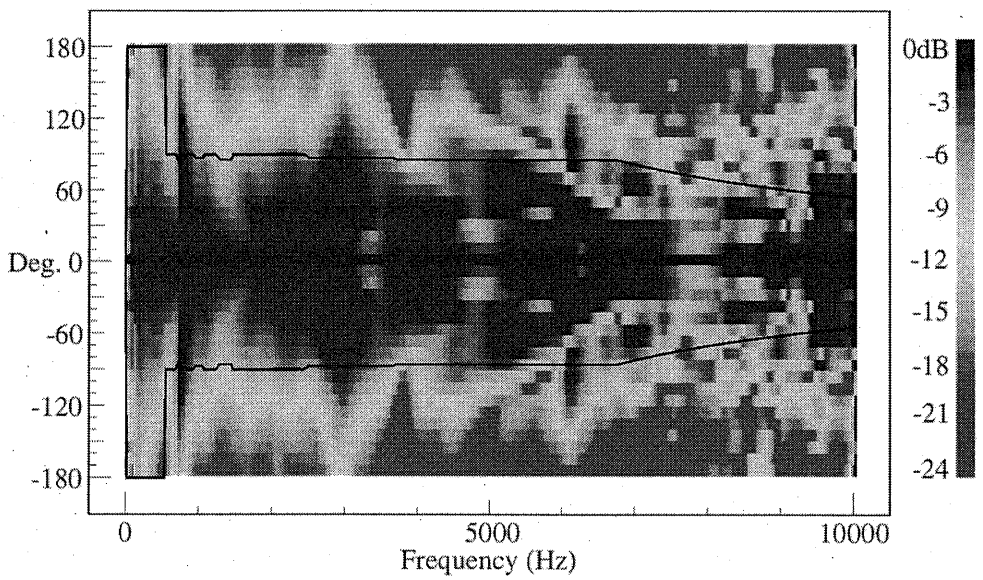

Figure 4a Measured horizontal off-axis frequency responses (colour contours) compared to model coverage-angle predictions (solid black lines): rectangular sectoral horn

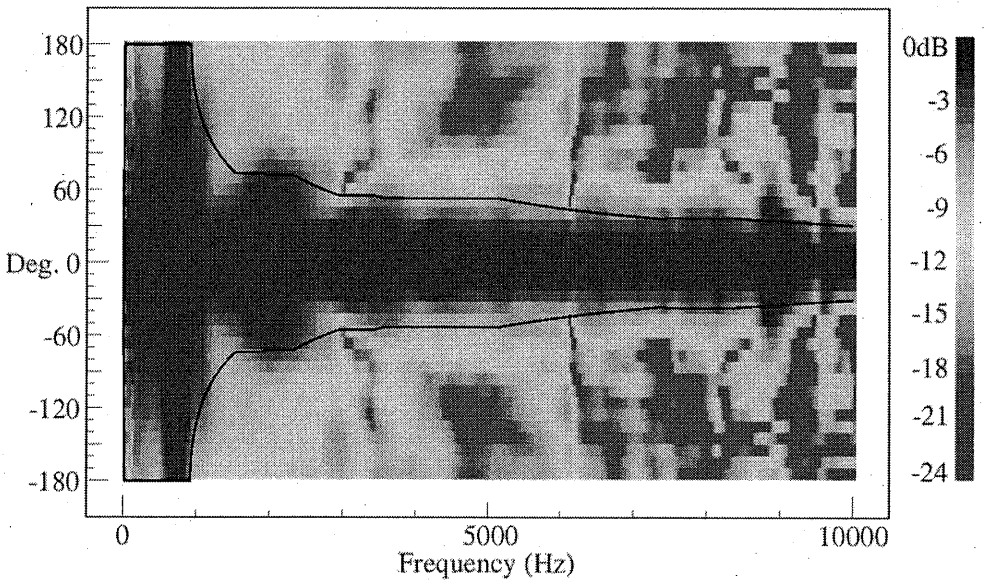

Figure 4b Measured vertical off-axis frequency responses (colour contours) compared to model coverage-angle predictions (solid black lines): rectangular sectoral horn

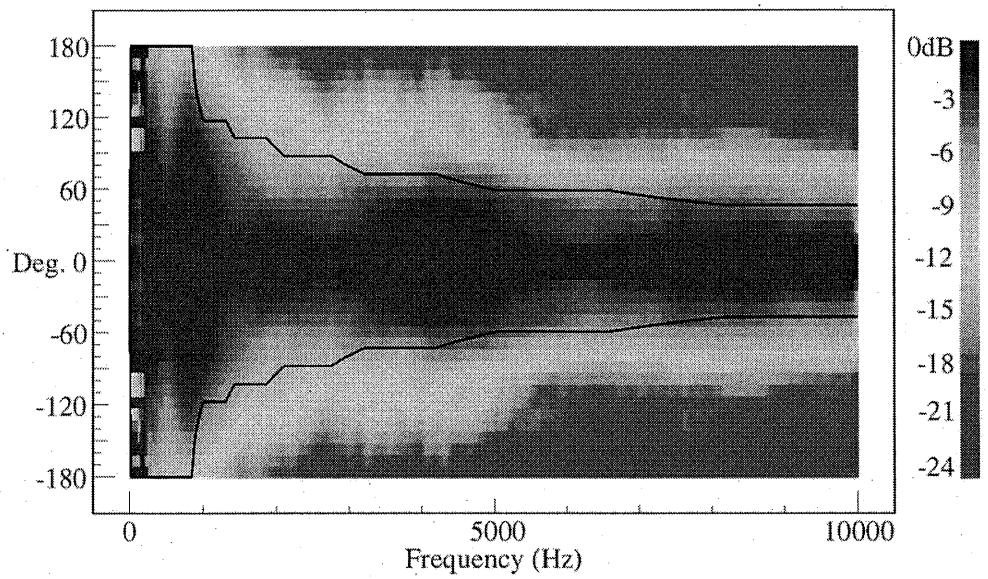

Figure 5 Off-axis frequency responses (colour contours) compared to model coverage-angle predictions (solid black lines): axisymmetric horn.

5 DISCUSSION AND CONCLUSIONS

The model proposed is efficient and compact compared to the more advanced numerical prediction tools such as finite element or boundary element models and can produce useful estimates of the coverage angle of horns. The examples used to verify the model show that those aspects of the coverage angle that are due to the horn walls are reasonably well captured, but that other horn features, such as blockages in the flare and non-ideal acoustic conditions at the mouth are not included in the predictions.

There are several applications of horn loudspeakers where the -3dB coverage angle (half power) may be more useful than the -6dB angle used here. If horns are used singly, rather than in arrays, and high-fidelity reproduction is desirable over a given angle, the -3dB coverage angle would better describe the high-fidelity coverage of the horn, although this angle is frequently not given in the manufacturers' specifications. An example of such an application would be the screen loudspeakers in cinemas. It is probable that a model similar to the one described in this paper could be developed to predict the-3dB coverage angle. This option, along with the inclusion of the mouth-narrowing, are suitable topics for further research.

6 REFERENCES

1. K R Holland, F J Fahy, C L Morfey and P R Newell, "The Prediction and Measurement of the Throat Impedance of Horns", *Proceedings of the Institute of Acoustics*, **11**(7), Reproduced Sound 5, 247-254, 1989.

2. K R Holland, F J Fahy and C L Morfey, "Prediction and Measurement of the One-Parameter Behaviour of Horns", *Journal of the Audio Engineering Society*, **39**(5), 1991.

3. K R Holland, "Measuring the Unknown Driver", *Proceedings of the Institute of Acoustics,* Reproduced Sound 16, 17-19 November 2000, **22**(16), 2000, 1-8.

4. T F Johansen, "On the Directivity of Horn Loudspeakers", *Journal of the Audio Engineering Society*, **42**(12), 1994.

5. L J Ziomek, *"Fundamentals of Acoustic Field Theory and Space-Time Signal Processing"*, CRC Press, 1995, ISBN: 0-8493-9455-4.

6. D B Keele, What's so Sacred About Exponential Horns? Presented at the 51st Convention of the Audio Engineering Society, May 1975.

7. C A Henricksen and M S Ureda, The Manta-Ray Horns. *Journal of the Audio Engineering Society*, **26**(9), 1978.

8. P R Newell and K R Holland, "*Loudspeakers for Music Recording and Reproduction*", 2nd Edition, Routledge, 2019, ISBN: 978-1-138-55480-1.

9. K R Holland, "*A Study of the Physical Properties of Mid-Range Loudspeaker Horns and their Relationship to Perceived Sound Quality*", PhD Thesis, University of Southampton, 1992.

7 APPENDIX

Pictures of the horns used to verify the model.

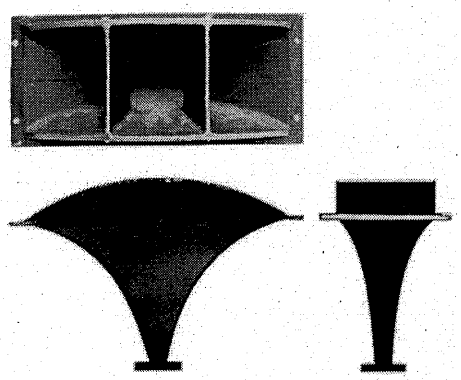

Figure A1 Rectangular exponential horn

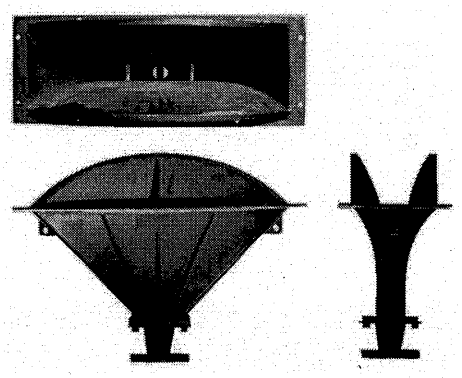

Figure A2 Rectangular sectoral horn. Note discontinuities within the flare.

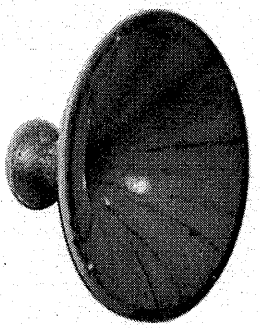

Figure A3 Axisymmetric horn

Proceedings of the Institute of Acoustics

ANOTHER LOOK AT THE RELATIONSHIPS BETWEEN FREQUENCY RESPONSE AND THE SPEECH TRANSMISSION INDEX, WITH RESPECT TO WORD SCORES AND ROAD TUNNELS

G. Leembruggen Acoustic Directions and ICE Design, Sydney Australia

1 INTRODUCTION

This paper takes another look at the relationships between frequency response and the speech transmission index (STI). Experience gained by the author and colleagues over many years of designing and commissioning sound systems has shown that a degraded frequency response can greatly reduce speech intelligibility. In reverberant, low noise environments, major degradation in responses can make speech essentially not understandable, and this loss of intelligibility is often barely reflected in the STI performance. Additionally, relatively small changes over an octave bandwidth, sometimes as small as 1 dB, can noticeably improve the perceived intelligibility of conversational speech and this change in perceived intelligibility is virtually not reflected in the STI.

Both of these situations suggest that the psychoacoustic masking mechanism that occurs with relatively low levels is not fully accounted for by the STI process.

Situations involving sound systems should allow listeners to understand speech without concentrating on the listening process itself. There are many situations (for example rail and bus terminals) which have sound systems meeting a specified STI performance, but in which listeners must concentrate to understand the speech, especially when that speech is delivered rapidly or with poor articulation. Other situations such as parliaments and courts are more demanding, requiring participants to listen for long periods and concentrate on the subject matter. These systems should not only deliver satisfactory speech intelligibility, but should provide "acoustic comfort" for listeners, so that they can actively engage with the speech without straining to understand the content. To achieve this robust intelligibility, the system must accurately reproduce the full range of voice types and speaking styles.

1.1 Part 1: Revisit of 2003 STI Work

The first section of this paper revisits work presented by the author and a colleague[1] in 2003 to the Reproduced Sound conference. That paper explored the apparent inability of the STI metric to properly account for the perceived loss of speech intelligibility that occurs with poor frequency response in public address situations, particularly in reverberant environments.

Measurements of STI were made in a reverberation chamber using a loudspeaker with seven frequency response scenarios. The scenarios were derived from seven sets of equalisation filters that were grossly different. Those STI results were compared with the equivalent STIs derived from word scores obtained from listening tests with recordings made in the same reverberation chamber with the same seven frequency responses. As the ambient noise levels were low in both the speech-recording and listening situations and there were negligible echoes in the reverberation chamber (compared to the reverberation), intelligibility degradation was only due to reverberation and the frequency-response filters. The shape of the filters was selected to represent a highly exaggerated situation, that would rarely be encountered in real-life public address situations.

The paper concluded was that in reverberant, noise free situations, STI measurements of situations with highly degraded frequency responses were essentially unable to match the equivalent STI from the word scores.

This paper uses the measured data from 2003 to revisit the relationship between measured and word-score STIs by addressing the following issues:

a) Critique from colleagues concerning the true ambient noise and listening levels during the word score tests.

   A range of ambient noise levels and spectra that could be more representative of the listening environments was therefore used in this analysis.

b) Application of the speech spectrum during the STI calculation, rather than applying a speech shaped filter to the actual test signal, which was the case in 2003. This provides a higher signal-to-noise ratio for the speech signal.

c) Application of the continuous auditory masking mechanism specified in STI standard IEC 60268-16 -2011[2] (Rev. 4).

d) The new relationship between phonetically-balanced word scores and STI for real-world listening between recently developed by Morales et al[3] et al.

1.2 Part 2: STI and Frequency Response in Two Road Tunnels

Part 2 of this paper continues the theme established in Part 1 concerning the comparative independence of frequency response and STI.

With the experience of designing and/or commissioning emergency sound systems for ten road tunnels in Australia and New Zealand, the author is aware that the specifications for emergency sound system performance in these types projects generally focus on STI, which is typically to be assessed in the presence of the smoke-exhaust jet-fans. Little regard seems to be given to the importance of frequency response and perceived intelligibility. A consequence of this focus on STI is that many tunnel systems provide very poor subjective intelligibility although they may just meet specification.

The author is also becoming increasingly concerned at the willingness of many audio and electro-acoustic practitioners to focus on the operational performance of systems, without any critical listening work to understand and optimise the subjective performance of the system.

In the context of these two concerns, the author considers it possible that when the acoustic performance of a tunnel system is being benchmarked after commissioning, if the system complies with or is close to the STI specification, the system will be regarded as "good enough", without regard for the perceived intelligibility and listening comfort.

It was therefore instructive to explore the effect of gross frequency response changes on the STI performance in the presence of jet-fan noise with two tunnels in New Zealand. These two tunnels were recently designed and commissioned by the author and the filters selected for this investigation would produce a very large degradation in the sound quality during emergencies compared to the sound without these filters.

2 PART 1

2.1 Overview of 2003 Work

2.1.1 Objective Measurements

An investigation was conducted into the relationship between the subjective intelligibility of speech and the measured STI for a range of frequency responses in a reverberant environment. The method consisted of measurements of the STI for each response, subjective testing of word scores for each response, and processing of the measured STI results and word scores.

A loudspeaker and dummy head with binaural microphones were set up in an anechoic chamber at AMS Acoustics. The loudspeaker was fed with an MLS signal via a speech-weighting filter and power amplifier. The response of the speaker was then measured at each ear using binaural microphones at a distance of 1.5 m from the speaker on axis and processed by MLSSA v10w

analyser to yield the anechoic frequency response of the speaker and the STI. This anechoic measurement is Scenario 1.

The loudspeaker was moved into a reverberation chamber at AMS Acoustics, and the STI was again measured at a distance of 1.5 m from the speaker on axis using binaural microphones. Using acoustic absorption material, the reverberation time of the chamber was adjusted so that the measured STI was approximately 0.5; this is Scenario 2. The measured reverberation times in the chamber are shown in Table 1.

Frequency	125	250	500	1000	2000	4000	8000
RT (secs)	3.5	3.3	2.2	1.7	1.7	1.4	1.1

Table 1 Measured reverberation times in the reverberation chamber with applied sound absorption material to produce an STI of approximately 0.5.

Seven different filters were then used sequentially to shape the frequency response of the loudspeaker (Scenarios 3 to 9) with the same arrangement of sound absorption material. For each filter, the impulse response was captured and the frequency response and STI of the system computed.

2.1.2 Subjective Measurements

A CD of anechoically recorded speech was prepared and consisted of 1000 carrier sentences and words arranged into 20 groups of 50 words. The words were spoken by a female voice artist, and were single syllable, phonetically balanced (PB) types from Harvard situated at the end of each sentence.

Following a similar process to the objective measurements in the anechoic and reverberation chambers, three groups of fifty words were played through the loudspeaker and recorded onto digital media using binaural microphones on the dummy head at a distance of 1.5 m from the speaker. Recordings made in the reverberation chamber were made with the same arrangement of sound absorption material as the objective measurements, with a total of seven scenarios being recorded corresponding to the seven response shaping filters. When the groups of words were exhausted, a reshuffled version of the lists was used.

The recordings of the nine scenarios were then distributed to listeners in the UK and Australia. In the UK, seven listeners evaluated all or part of the three lists for each of the nine scenarios, to give a total of 135 listening sessions. In Australia, three listeners evaluated all three lists for each of the nine scenarios, to give a total of 81 listening sessions. The sentences were presented to listeners through headphones or loudspeakers, and the listener wrote down the word at the end of the sentence. The ambient noise level in the listening areas was relatively low, and typical of a living room environment.

2.2 Test Scenarios and Frequency Response Filters

The responses of the tonal filters were chosen from our experience to grossly exaggerate the difficulties for perceived intelligibility. Table 2 lists the environment and filters pertinent to each scenario. The frequency responses of the loudspeaker when fed with the filter and the responses of the filter itself are given in the Appendix.

Scenario	**Description**	**Tonal Filter**
1	anechoic	None
2	reverberant	None
3	reverberant	5 dB/octave cut
4	reverberant	5 dB/octave boost
5	reverberant	2.5 kHz 12dB notch Q=0.7

Scenario	Description	Tonal Filter
6	reverberant	Plateau @-3dB 400Hz to 1 kHz, plateau @ -10 dB 1.2kHz to 6 kHz
7	reverberant	250 Hz 18 dB boost Q = 1.5
8	reverberant	630 Hz 18 dB boost Q = 1.5
9	reverberant	Notches: 500 Hz & 2 kHz -18 dB

Table 2 Details of temporal and filter parameters for each scenario.

2.3 Computation of STIs with Refined Parameters

To compute the STIs for the conditions under which the word scores were obtained, a two-part process was used in accordance with the method laid out in Annex M of [2].

- In Part 1 of the process, the MTF data obtained using the MLSSA analyser was corrected to remove the effect on the STIs of ambient noise and masking computed by MLSSA. This process yielded MTF matrices that included degradation only by temporal effects, and hearing threshold.
- In Part 2, adjustments to the corrected MTF matrix were made for new ambient noise and listening levels and the masking algorithm specified in Rev 4 of the STI standard.

2.3.1 Listening Conditions

Five possible ambient noise levels for the listening situations were used for the STI calculations. An air-conditioned environment is assumed with noise levels ranging from a typical low-noise situation to an unlikely high-noise situation. The octave band L_{eq} levels corresponding to the five noise situations are shown in Table 3 and Figure 1.

Noise Situation	Frequency Hz							
	dBA	125	250	500	1000	2000	4000	8000
AC Low	32.3	36	34	29	27	22	18	15
NR 25	33.3	44	35	29	25	22	20	18
AC High	36.3	46	38	32	30	26	20	20
NR 30	38.0	48	40	34	30	27	25	23
NR 35	42.8	52	45	39	35	32	30	28

Table 3 Possible noise levels for the listening situation applied to the STI calculations.

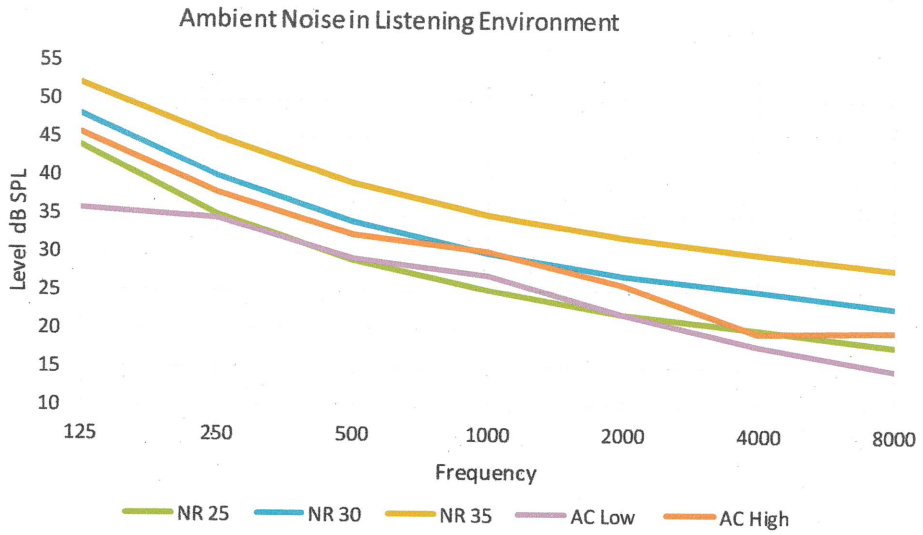

Figure 1 Spectra of the range of ambient noise levels applied to the listening environment.

The speech level for the STI calculations was set to 66 dBA, which is a comfortable level for speech in a small environment that would be regarded as quiet and suitable for critical listening. The male speech spectrum presented by Cushing et al[4] was used for the calculations as it has greater similarity to spectra measured by the author, Byrne et al[5], and the ANSI standard S3.5[6], compared to the spectrum specified by the STI standard.

The overall level of each filtered speech signal was adjusted (normalised) to 66 dBA. Figure 2 and Figure 3 show the octave band levels after normalisation with two alternative views to assist visualisation of the differences in the filtered spectrum.

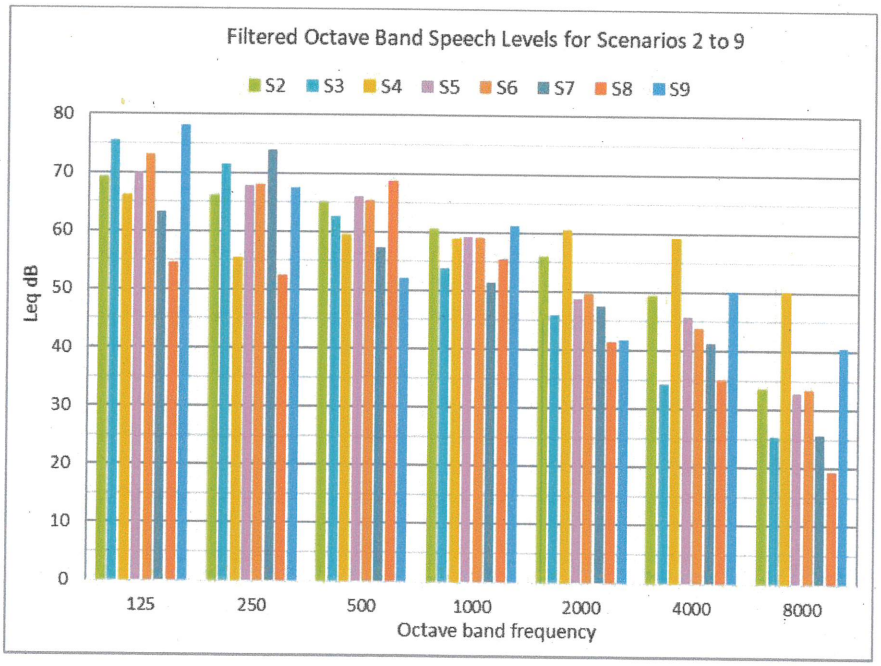

Figure 2 Octave band levels of speech when filtered with Scenarios 2 to 9 (frequency is abscissa).

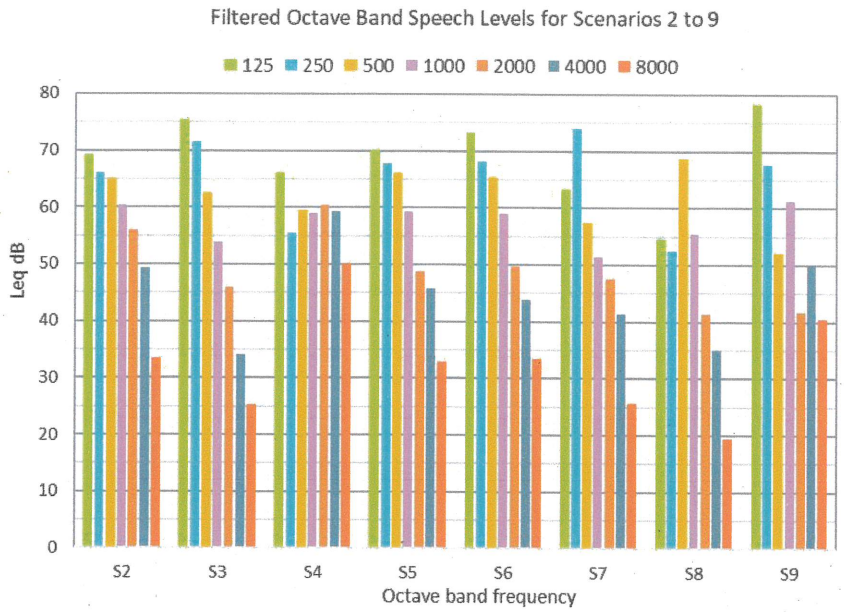

Figure 3 Octave band levels of speech when filtered with Scenarios 2 to 9 (Scenario is abscissa).

2.3.2 STI Results

The MTF matrix for the left ear was used for the STI calculations, as this ear gave the highest measured MTF values in the reverberation chamber. Table 4 shows the computed STIs for each filter scenario.

Filter scenario	AC Low 32.3 dBA	NR 25 33.3 dBA	AC High 36.3 dBA	NR 30 38.0 dBA	NR 35 42.8 dBA
2	0.52	0.52	0.52	0.52	0.51
3	0.51	0.51	0.50	0.49	0.46
4	0.51	0.51	0.51	0.51	0.50
5	0.52	0.52	0.52	0.51	0.50
6	0.53	0.53	0.52	0.52	0.51
7	0.50	0.49	0.49	0.48	0.46
8	0.49	0.48	0.47	0.46	0.42
9	0.52	0.52	0.52	0.52	0.50

Table 4 STI result for each filter scenario and ambient noise level for a listening level of 66 dBA.

2.4 Estimated STI from Word Scores

Figure 4 shows the word scores for both the UK and Australian listeners.

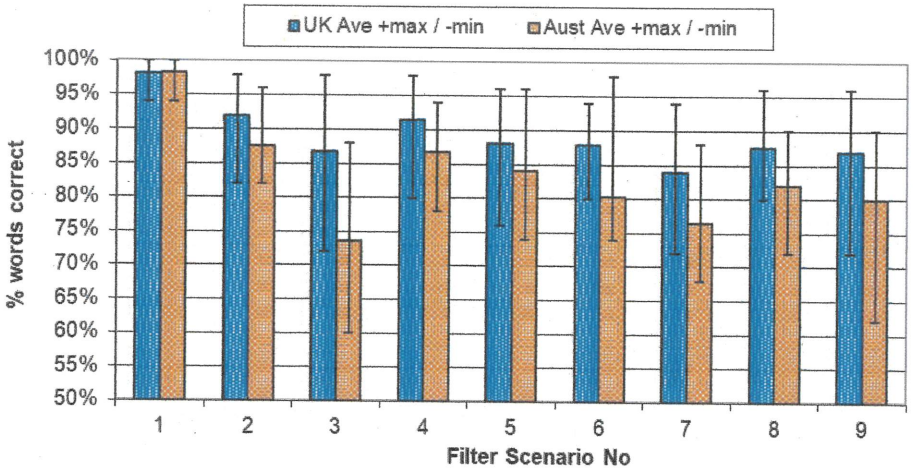

Figure 4 Plot of word score vs filter scenario. The error bars indicate the maxima and minima.

The following points are pertinent to the results.

a) Although the word score testing was not carried out rigorously in accordance with the ISO TR 4870 standard, and there was a wide range in the results, the trends were clear.

b) The average Australian scores for each scenario were generally lower than the corresponding UK scores. Judging by the difficulty the author has with the intelligibility with some BBC television productions, it is concluded that this difference was likely to result from accent differences.

c) There was a noticeable reduction in the word score when the tonal filters were inserted.

d) Even though the test words were well-articulated, each Australian listener found it necessary to concentrate while listening in order to discern the test words. More concentration was required for the filtered words. If this concentration had not been applied and the words had not been so well articulated in the original recording, the scores would have been lower.

e) Overall, the Australian listeners found the process to be quite tiring.

2.5 Associated STI Results

In 2003, the equivalent STIs were computed from the word scores using the relationship between phonetically-balanced words and STI published in 1985 by Anderson and Kalb[7] (AK). That relationship is presented in Figure E1 of Annex E in both the 2003 (Rev 3) and 2011 versions of standard 60268-16. Using a different experimental method to AK, Morales et al revised the relationships between the intelligibility of Harvard PB words and STI for real-world listening in both reverberant and noisy environments.

The relationships between the STIs and real-life listening presented by Morales et al were published between 2012[8] and 2018[9]. Refs [3] and [5] present relationships for reverberant situations only, whereas Ref [6] presents relationships for degradation due to combinations of reverberation, echoes, additive noise and bandpass limiting. As this assessment relates to reverberation only, Morales' relationship between the monaural measured STI and the average scores of the real-life PB word intelligibility tests shown in Figure 4 of [3] is used. Figure 5 below shows this relationship along with averaged PB score results for reverberation distortions from AK shown in Figure E1 of 60268-16 2011.

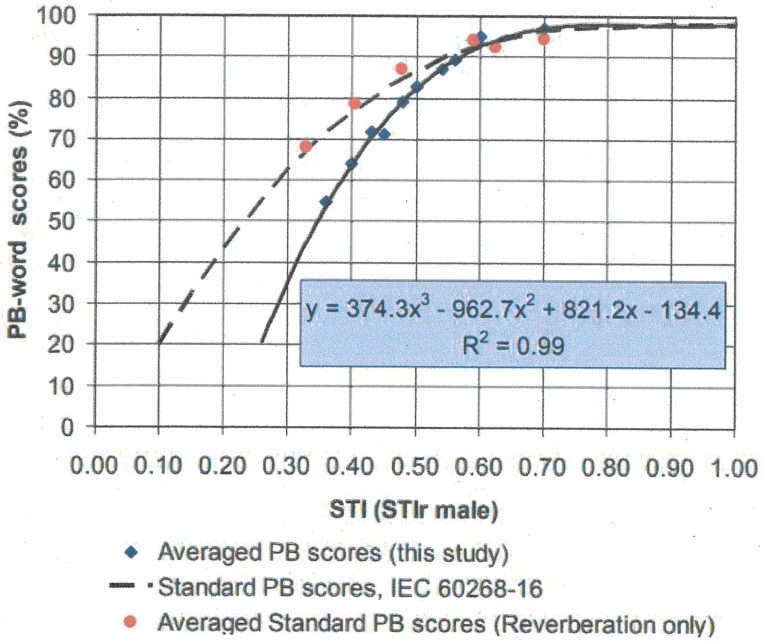

Figure 5 Relationship between the monaural measured STI and the average PB scores.

Table 5 presents the STI results for each scenario in the estimated listening situation.

Scenario	Equivalent STI from Word Score		Description	Tonal Filter
	UK	Aust		
1	0.82	0.83	anechoic	None
2	0.60	0.55	reverberant	None
3	0.54	0.45	reverberant	5 dB/octave cut
4	0.59	0.54	reverberant	5 dB/octave boost
5	0.55	0.52	reverberant	2.5 kHz 12dB notch Q=0.7
6	0.55	0.49	reverberant	Plateau -3dB 400 Hz to 1 kHz Plateau -10 dB 1.2 kHz to 6 kHz
7	0.52	0.47	reverberant	250 Hz 18 dB boost Q = 1.5
8	0.55	0.50	reverberant	630 Hz 18 dB boost Q = 1.5
9	0.54	0.49	reverberant	Notches 500 Hz & 2 kHz -18 dB

Table 5 Computed STI results for each scenario in the estimated listening situation.

Figure 6 compares the equivalent STIs for the UK and Australian word scores and the measured STIs for each filter scenario and noise situation. The maximum and minimum of the word-score STIs are also indicated. Although the STI for NR35 is included for completeness, the author considers it is unlikely that this noise spectrum would have been present when the word scores were obtained.

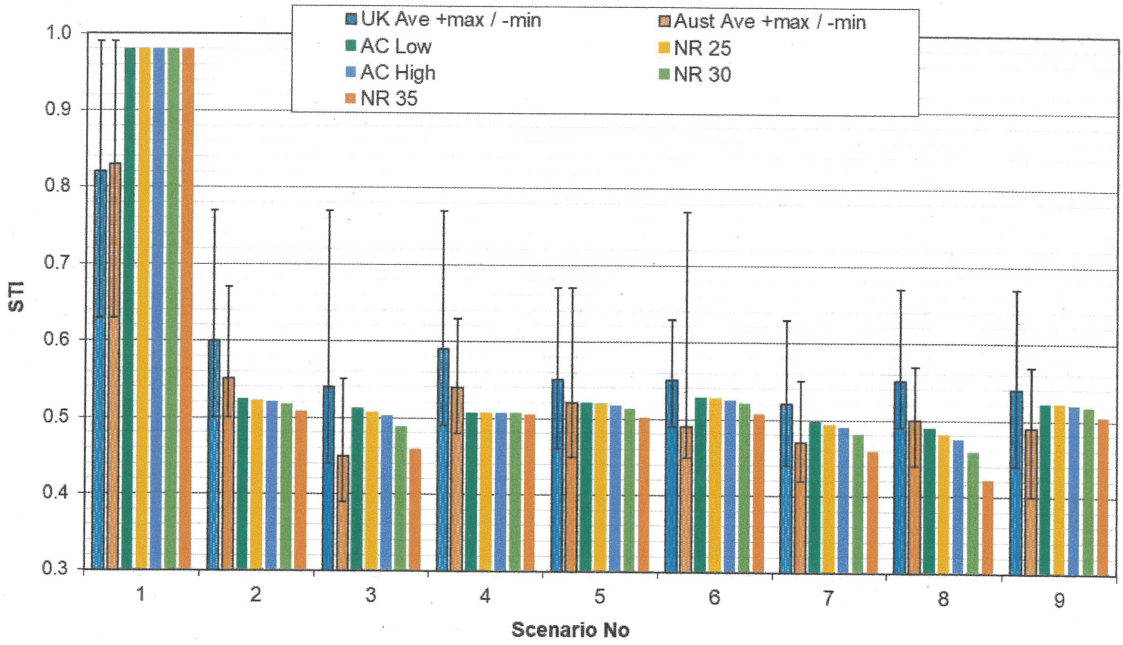

Figure 6 Comparison of equivalent STIs from word scores and measured STI vs filter scenario for the five noise situations. The error bars indicate the maxima and minima.

2.6 Discussion

The following points are noted, and for the reason noted above, the NR35 ambient noise situation is not included as it represents an unlikely listening scenario.

a) If the words had not been spoken by a voice artist with good articulation, the word scores would have likely been lower.

b) The STIs for Scenario 2 are relatively close (within 0.02) to the minimum equivalent STI for the Australian listeners.

c) With filter Scenarios 3, 6, 7 and 9, the measured STIs are lower than the Australian average, whereas for Scenarios 2, 4, and 8, the measured STIs are higher than the Australian average. The measured STIs in Scenario 5 are close to the Australian average. However, Scenario 8 is an unusual case as it is a narrow peaking boost of 20 dB at 630 Hz.

d) Other than the NR30 situation and Scenario 8, none of the STIs for the filter scenarios and noise situations is able to satisfactorily mirror the minimum STI scores of the Australian listeners, particularly at the lower ambient noise levels. This result highlights the need to recognise that more words could be lost than suggested by the average STI relationship developed by Morales.

e) Figure 7 shows an expanded view of Morales' relationship between word score and equivalent STI in reverberation-only situations, with the axes reversed. When viewed in this form, it is more readily recognised that a loss in PB words of 5% to 40% covers only a range of 0.25 in STI.

In terms of the general awareness of STI users, the range of 0.64 to 0.39 is within a familiar range. What may be more unfamiliar is that this range encompasses such a large extent of lost words. Given that complex instructions or unfamiliar words could be regarded as having some similarity to PB words in their degree of difficulty for recognition, this potential loss in word recognition is much greater than the STI value suggests.

f) Morales' relationship assigns a given loss of intelligibility to a higher STI than the AK relationship. For example, Morales equates a 40% loss of PB words to an STI of 0.39 compared to AK's STI of 0.29. Morales' relationship therefore compresses the range of word losses into a smaller STI range with higher absolute values than before. As such, an organisation wishing to approve a given STI performance based on a limited understanding of STI would approve the result without an understanding of the potential loss of intelligibility, particularly with respect to unfamiliar words.

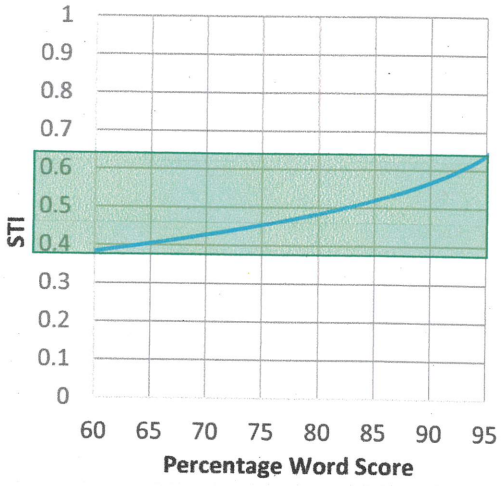

Figure 7. Expanded view of reversed relationship between STI and word score.

g) A primary difficulty is that no STI verification has been done for speech in which the tonal structure within the 250 Hz to 4 kHz has been highly distorted. As such, Morales' relationship may not properly represent the loss of intelligibly that occurs with self-speech masking when the frequency responses are poor.

h) The measured STI values are based on a long-term average speech spectrum, whereas the spectra of individual words can show significant differences with that average spectrum. This is illustrated in Figure 8, which shows the difference between the standardised IEC speech spectrum and the spectra of five PB words used in the 2003 work. Differences of up to 20 dB are evident. The possibility of self-speech masking becomes much more likely during words with soft consonants at the end such as "salve", "sheik", "quip" and "dung" with this type of spectra. The self-masking that can occur with these types of words is essentially not recognised by STI's masking algorithm.

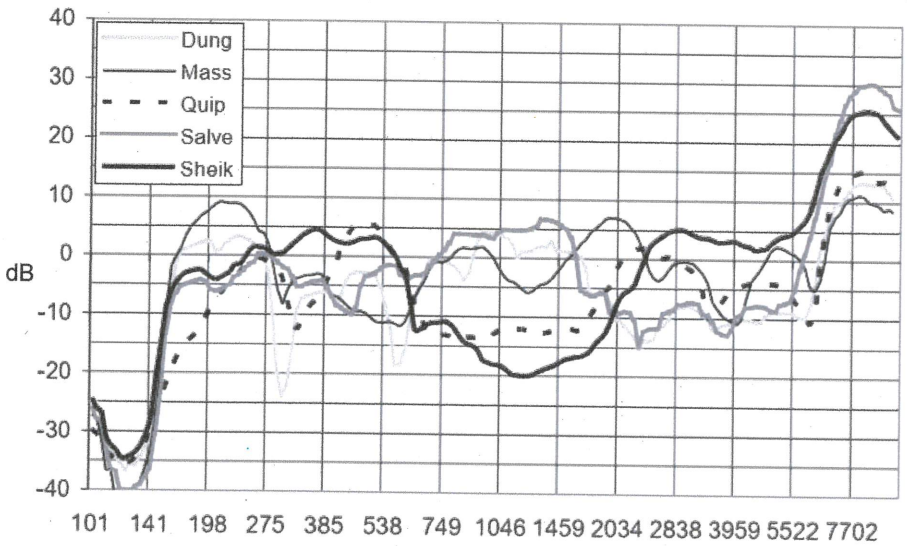

Figure 8 Differences in the spectra of five PB words and the standard IEC speech spectrum.

i) As a "broad brush" approach, the measured STI results appear to reasonably represent the word scores. However, when the receipt by listeners of critical information is at stake and the talkers are not trained actors, the broad brush of STI is not able to satisfactorily quantify the actual loss of intelligibility.

3 PART 2

3.1 Site Work

The electro-acoustic optimisation process of each road tunnel sound system consisted of equalisation, setting signal delays and optimising the gain structure of the system.

a) A suitable equalisation was developed using a combination of acoustic measurements and listening to optimise subjective speech intelligibility, naturalness of tone, and listening comfort at high levels.

When listening to speech at levels exceeding 90 dBA, strong high-frequency content such as occurs in sibilant words, can rapidly become very uncomfortable. As good high-frequency response is also essential for speech intelligibility, the approach we used was a combination of a slight reduction in the equalised response above 5 kHz, and careful de-essing of specific words, which was generally those words ending in the letter 's'.

b) A goal of the work to develop the gain structure of the system so that the long-term L_{Aeq} level was as high as possible in order to maximise the STI, whilst ensuring that the system did not produce strongly audible distortion. The gain structure was developed using a combination of broadband level measurements, capturing the amplifier output using a digital oscilloscope and critical listening.

To achieve this outcome, a crest factor of 21 dB needed to be provided. At face value this crest factor seems excessive but is required to accommodate the necessary high-frequency equalisation boost of 22 dB at 11 kHz. Although the long-term RMS level of speech was low, short-term peaks in this frequency range can be up to 21 dB above the long-term overall RMS level.

c) As amplifiers in road tunnel systems can be of variable quality and often do not overload (clip) cleanly, distortion can be clearly audible even with modest amounts of clipping. In this context. care is required to ensure distortion is not particularly audible.

After the sound system in each tunnel was optimised for perceived intelligibility and tonal comfort, the performance of the system was benchmarked using the direct STI method STIPA. In Tunnel 1 (VPT), measurements were made at 58 locations along its 410 m length, while in Tunnel 2 (JHT), measurements were made at 47 locations along its 320 m length.

The level of the STIPA signal was carefully set so that its spatially-averaged level was equivalent to the spatially-averaged level of speech. To achieve this, the STIPA level was set 2 dB higher than the speech level to account for the reduction in long-term speech level that gaps between words produce. That reduction was computed from the speech audio file as the difference in RMS levels between the announcement with gaps and without gaps.

Measurements were also made in octave bands of the noise produced by the smoke-exhaust jet-fans in the tunnels. Figure 9 shows the total L_{Aeq} sound pressure level of the fan noise expressed as $L_{Aeq\text{-}1second}$ along VPT (northerly direction) and JHT (southerly direction). Each one-second interval produced a spatial average of the sound levels over a traversed distance of approximately 1 m.

The STIPA measurements at each position provided i) the level in octave bands of the test signal shaped to the standard IEC speech spectrum and ii) the MTF matrix. Using a bulk calculation process, the jet-fan noise was introduced into each STIPA measurement. That process also incorporates the masking and threshold calculations and follows the method of Annex M in [2]. Table 6 shows the averages and standard deviations of the STI performance with and without jet-fan noise and the equivalent L_{Aeq} level of speech in the tunnel.

Neither of the two systems can be regarded as optimally designed, as the project brief was to make improvements to the existing systems by changing only the loudspeakers and cabling. No additional amplifiers were to be installed. This constraint resulted in distances between loudspeakers that would normally be regarded as large in the case of VPT and very large in JHT.

	VPT		
	STI with noise	STI without noise	Speech L_{Aeq}
Average	0.48	0.51	93.5
Std Dev	0.07	0.05	1.19

	JHT		
	STI with noise	STI without noise	Speech L_{Aeq}
Average	0.38	0.45	92.0
Std Dev	0.05	0.05	1.5

Table 6 STI results in the two tunnels measured during the benchmarking process.

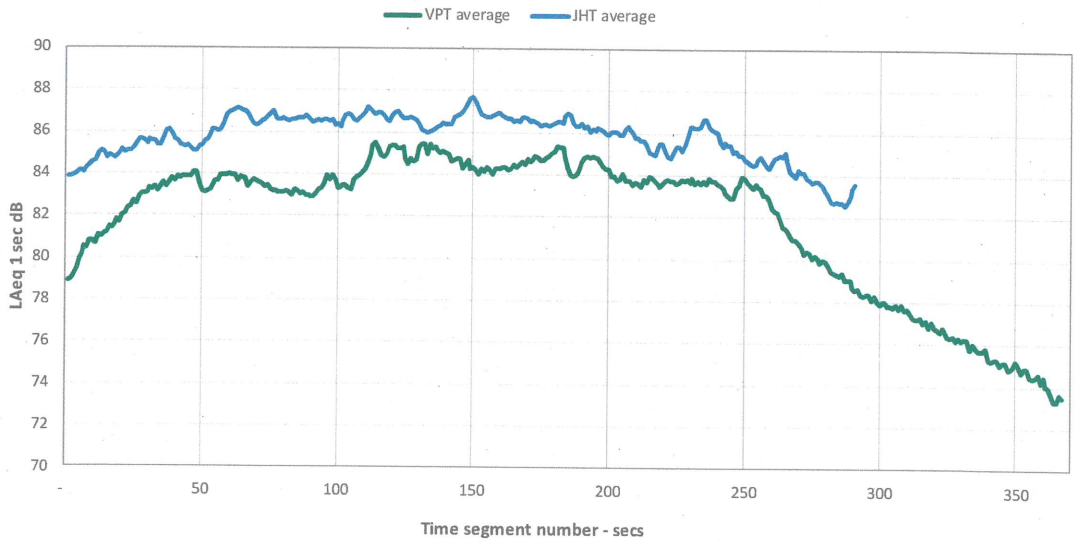

Figure 9 Broadband noise levels along the two tunnels.

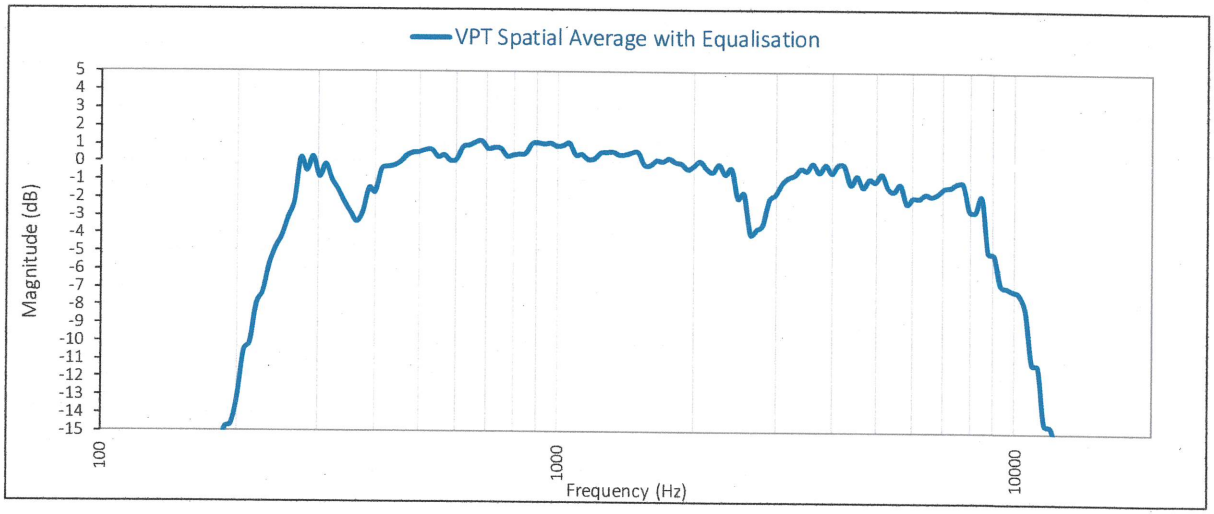

Figure 10 Example of spatially-averaged frequency response after equalisation and optimisation of the perceived intelligibility and listening comfort.

3.2 Effect of Changes to Frequency Response on the STI

3.2.1 Frequency Responses Used

To assess the change in STI performance resulting from a change in the frequency response of the system for this paper, six different filters were applied in bulk to the STI calculations for each tunnel. These filters were selected to demonstrate the insensitivity of the STI results to changes in frequency response that would sound extremely poor and would result in highly degraded

intelligibility. The filters took the form of boosts or cuts to a number of octave bands. Table 7 shows the levels in each octave band for the applied filter.

As the boost or cuts affect the overall level of the speech signal in the calculations, an overall level adjustment was applied so that the L_{Aeq} of the speech signal remained constant. To illustrate the octave band levels in Table 7 that would result with filtered pink noise, Figure 11 provides a graphical examples of frequency response that produce the octave band levels in each filter response. Subjective descriptions are also given.

Filter No	Octave Band Frequency Hz							Overall level adj.
	125	250	500	1000	2000	4000	8000	
1*	0	0	0	0	0	0	0	0
2	0	0	0	-3	-3	-3	-5	1.2
3	0	4	2	-4	-4	0	0	-0.6
4	0	0	0	2	-5	-2	0	-0.2
5	0	0	-4	2	-4	-4	0	1.0
6	0	0	0	-9	-9	0	0	1.9
7	0	0	0	-6	0	6	0	0.2

Table 7 Octave band levels applied to shape the frequency responses in the tunnels. All values are in dB. *Existing response without filter.

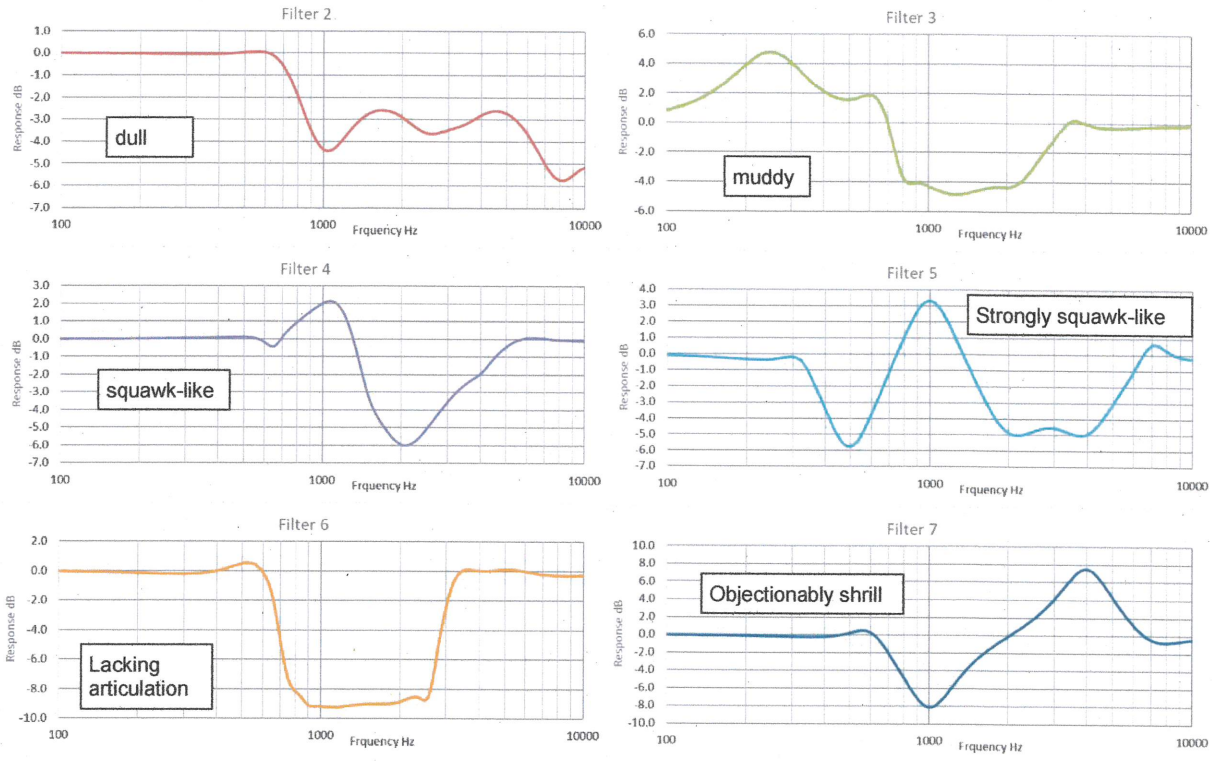

Figure 11 Example frequency responses that produce the octave band levels in Table 7 with pink noise. Subjective descriptions are also given.

3.2.2 STI results

	VPT			JHT		
Filter No	Average STI	Std Dev	Change in STI	Average STI	Std Dev	Change in STI
1*	0.48	0.07		0.38	0.05	
2	0.46	0.07	0.02	0.36	0.05	0.02
3	0.45	0.07	0.03	0.35	0.05	0.03
4	0.44	0.07	0.04	0.36	0.05	0.02
5	0.45	0.07	0.03	0.36	0.05	0.02
6	0.43	0.07	0.05	0.34	0.05	0.04
7	0.47	0.06	0.01	0.37	0.04	0.01

Table 8 Average STIs and standard deviations for the two tunnels with the actual response (No 1*) and six shaping filters.

Table 8 shows the STI results with the filters inserted into the calculations. Inspection of the results reveals that significant reductions in the sound energy within octave bands that are deemed more critical for intelligibility (1 kHz to 8 kHz) have only minor effects on the STI, even during situations with high noise levels.

The author concludes that when specifying or commissioning an emergency sound system in a road tunnel, blind adherence to simply achieving a STI performance without paying significant attention to the frequency response of the system over the entire listening area, can yield a system which produces poor perceived intelligibility and yet its performance meets the project specification.

4 REFERENCES

1 Leembruggen, G.A, Stacy A. Should the Matrix be Reloaded? Proc IOA. 2003

2 IEC. Sound System Equipment Part 16: Objective rating of speech intelligibility by Speech Transmission Index. 3rd Edition, 2011. International Standard No. 60268-16

3 Morales, L; Dance, S; Shield, B; Leembruggen, G. Speech Transmission Index for the English Language Verified Under Reverberant Conditions with Two Binaural Listening Methods: Real-Life and Headphones. J. Aud. Eng. Soc. Vol 62 Issue 7/8 pp. 493-504; July 2014

4 Cushing, Li, Cox, Worral, Jackson. Vocal effort levels in anechoic conditions. Applied Acoustics. 2011, Vol. 72, pp. 695-701

5 Byrne, et al. An international comparison of long-term average speech spectra. JASA 1994, Vol. 96

6 ANSI. Methods for Calculation of the Speech Intelligibility Index. American National Standard. S3.5-1997

7 Anderson, B.W., and Kalb, J.T. "English verification of the STI method for estimating speech intelligibility of a communications channel," J. Acoust. Soc. Am. Vol 81, 1987, pp 1982-1985f

8 Morales, L; Dance, B; Leembruggen, G, Preliminary validation of the revised STI male for the English Language. Proc IOA Vol 34 Pt 4 2012

9 Morales, L; Li, F A new verification of the speech transmission index for the English language. Speech Communication 105 (2018) 1–11

APPENDIX FREQUENCY RESPONSES OF FILTER SCENARIOS

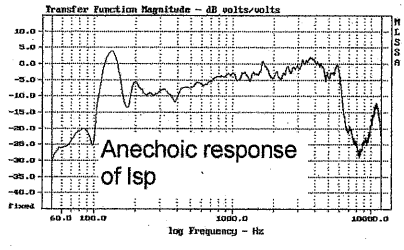

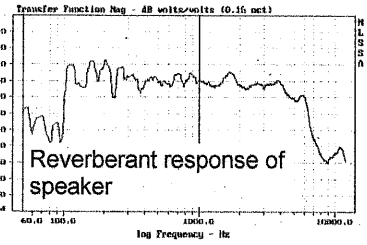

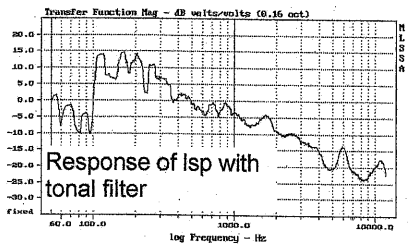

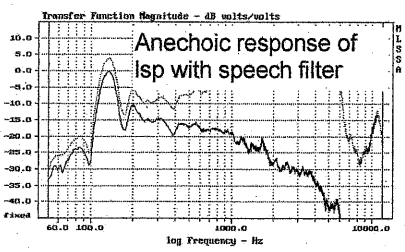

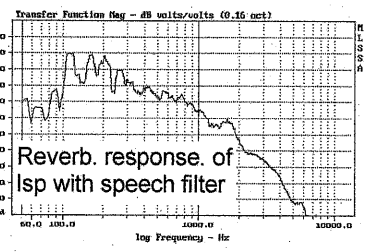

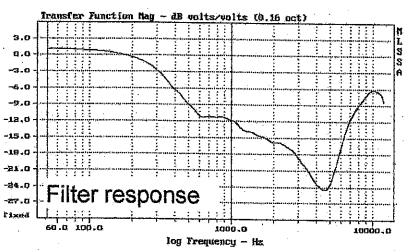

Scenario 1 **Scenario 2** **Scenario 3**

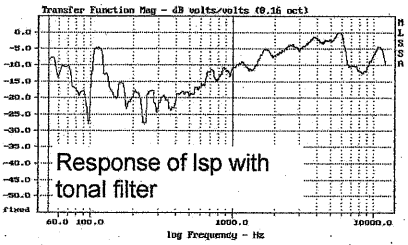

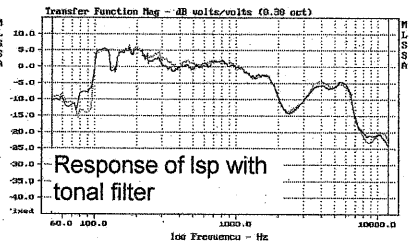

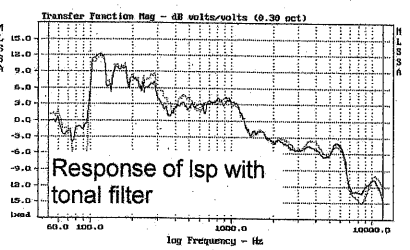

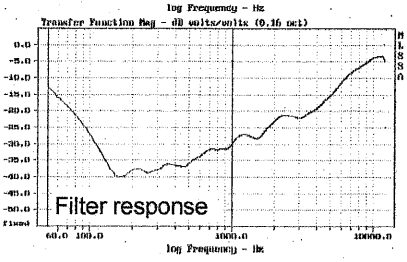

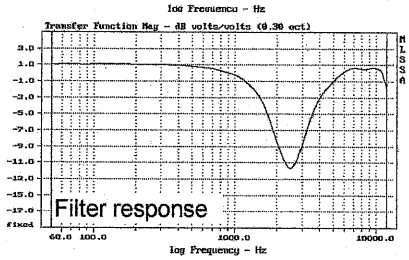

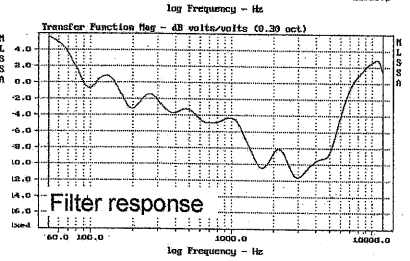

Scenario 4 **Scenario 5** **Scenario 6**

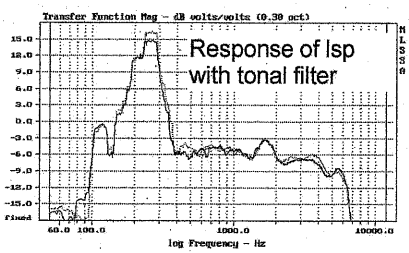

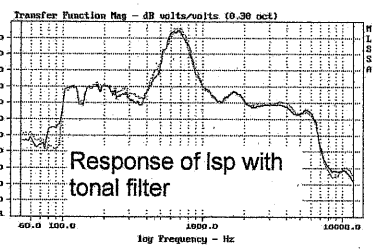

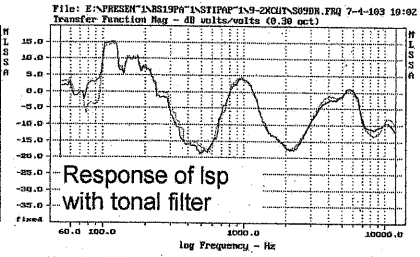

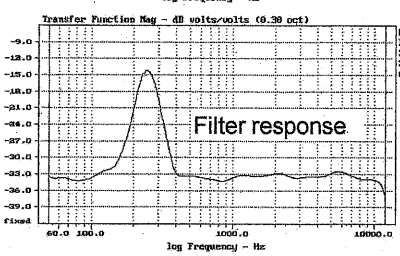

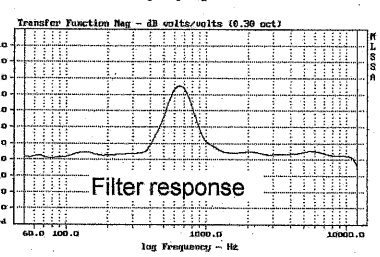

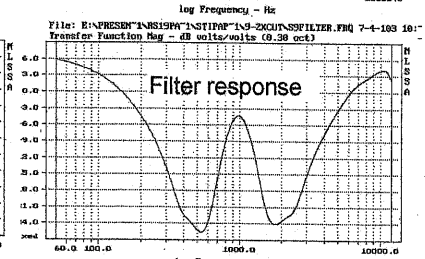

Scenario 7 **Scenario 8** **Scenario 9**